The Partial Hydrogenation of Benzene to Cyclohexene by Nanoscale Ruthenium Catalysts in Imidazolium Ionic Liquids

Edson T. Silveira,[a] Alexandre P. Umpierre,[a] Liane M. Rossi,[a] Giovanna Machado,[a] Jonder Morais,[b] Gabriel V. Soares,[b] Israel J. R. Baumvol,[b] Sergio R. Teixeira,[b] Paulo F. P. Fichtner,[c] and Jairton Dupont*[a]

Abstract: The controlled decomposition of an Ru^0 organometallic precursor dispersed in 1-*n*-butyl-3-methylimidazolium hexafluorophosphate (BMI·PF_6), tetrafluoroborate (BMI·BF_4) or trifluoromethane sulfonate (BMI·CF_3SO_3) ionic liquids with H_2 represents a simple and efficient method for the generation of Ru^0 nanoparticles. TEM analysis of these nanoparticles shows the formation of superstructures with diameters of ≈ 57 nm that contain dispersed Ru^0 nanoparticles with diameters of 2.6 ± 0.4 nm. These nanoparticles dispersed in the ionic liquids are efficient multiphase catalysts for the hydrogenation of alkenes and benzene under mild reaction conditions (4 atm, 75 °C). The ternary diagram (benzene/cyclohexene/BMI·PF_6) indicated a maximum of 1% cyclohexene concentration in BMI·PF_6, which is attained with 4% benzene in the ionic phase. This solubility difference in the ionic liquid can be used for the extraction of cyclohexene during benzene hydrogenation by Ru catalysts suspended in BMI·PF_6. Selectivities of up to 39% in cyclohexene can be attained at very low benzene conversion. Although the maximum yield of 2% in cyclohexene is too low for technical applications, it represents a rare example of partial hydrogenation of benzene by soluble transition-metal nanoparticles.

Keywords: biphasic catalysis · hydrogenation · ionic liquids · nanoparticles · ruthenium

Introduction

Multiphase transition-metal catalysis can combine advantages of both classical homogeneous and heterogeneous processes, such as catalyst recycling, product separation, mild reaction conditions and modulation of catalyst properties.[1] Indeed, these properties are nowadays largely explored in both academia and industry mainly by the use of aqueous[2] and ionic liquid[3] phase organometallic and colloidal catalysis.[4] Moreover, in these multiphase processes, primary products can be extracted during the reaction to modulate the product selectivity (playing with different substrates and reaction products solubility with the catalyst-containing phase). Indeed, this approach can constitute a suitable method to avoid consecutive reactions of primary products and it has been exploited to some extent in aqueous-phase catalytic processes. For example, the selectivity in primary amines was successfully controlled in aqueous-phase palladium-catalysed telomerisation of butadiene with ammonia in which the formation of secondary amines was reduced to less than 2%.[5] More importantly, the selective hydrogenation of benzene to cyclohexene can be successfully achieved by the use of nonsupported ultrafine ruthenium catalysts suspended in an aqueous phase, usually in the presence of additives.[6,7] Surprisingly, this method has been rarely exploited in multiphase ionic liquid catalysis. In only two cases was the reaction selectivity (hydrogenation of dienes to monoenes) attributable to differences of substrate and product solubility in the ionic liquid, catalytic phase.[8] Moreover, it is well-known that the solubility of organic compounds in 1,3-dialkylimidazolium ionic liquids can be modulated by simple changes in *N*-alkyl imidazolium substituents and/or in the anion. In particular, benzene is highly soluble in the 1-*n*-butyl-3-methylimidazolium hexafluorophosphate ionic

[a] M.Sc. Chem. E. T. Silveira, Dipl. Chem. Eng. A. P. Umpierre, Dr. L. M. Rossi, Dr. G. Machado, Prof. Dr. J. Dupont
Laboratory of Molecular Catalysis
Institute of Chemistry, UFRGS, Av. Bento Gonçalves
9500 Porto Alegre 91501-970 RS (Brazil)
Fax: (+55) 5133167304
E-mail: dupont@iq.ufrgs.br

[b] Prof. Dr. J. Morais, Dipl. Phys. G. V. Soares, Prof. Dr. I. J. R. Baumvol, Prof. Dr. S. R. Teixeira
Institute of Physics, UFRGS, Av. Bento Gonçalves
9500 Porto Alegre 91501-970 RS (Brazil)

[c] Prof. Dr. P. F. P. Fichtner
Department of Metallurgy, UFRGS, Av. Bento Gonçalves
9500 Porto Alegre 91501-970 RS (Brazil)

Supporting information for this article is available on the WWW under http://www.chemeurj.org/ or from the author. This information includes XRD and XPS spectra and TEM micrographs of the Ru nanoparticles.

DOI: 10.1002/chem.200305765

liquid at room temperature, whereas alkenes and alkanes are sparingly soluble.[9] Therefore, imidazolium ionic liquids could constitute an alternative media for the selective hydrogenation of benzene to cyclohexene. It is also reasonable to assume that the ionic liquid can act as a modifier of the metal catalyst, thus repelling the cyclohexene formed and decreasing the re-adsorption and further hydrogenation to cyclohexane. Herein we report our results concerning the partial hydrogenation of benzene by supported and nonsupported ruthenium catalysts in the ionic liquid 1-*n*-butyl-3-methylimidazolium hexafluorophosphate (BMI·PF_6). Furthermore, we have also determined the ternary diagram of benzene/cyclohexene/BMI·PF_6 ionic liquid and investigated the formation and stabilisation of nanoscale Ru^0 particles in the ionic liquid.

Results and Discussion

Benzene/cyclohexene/BMI·PF_6 ternary mixture: The room-temperature solubilities of benzene and cyclohexene in BMI·PF_6 are 37 and 6 wt%, respectively.[9,10] However, in order to determine the benzene and cyclohexene contents in the ionic liquid phase under the catalytic reaction conditions, we investigated the different compositions of benzene, cyclohexene and cyclohexane in the organic and ionic phases at 75 °C by gravimetric methods. The results are presented in Figures 1–3.

The solubility of benzene in BMI·PF_6 at 75 °C is lower than that determined at room temperature.[9] It is clear from the data in Figures 1 and 2 that the maximum concentration of cyclohexene (~1%) in the ionic liquid phase is attained when the benzene concentration is ≈4%. Moreover, with benzene concentrations greater than 34%, the content of cyclohexene is negligible in the ionic liquid phase.

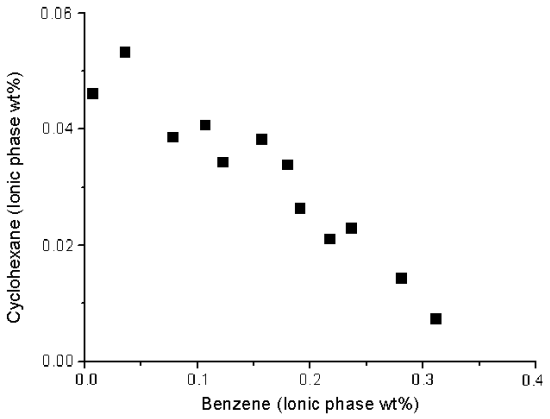

Figure 1. Benzene and cyclohexane contents in the ionic phase at 75 °C in a benzene/cyclohexane/BMI·PF_6 mixture.

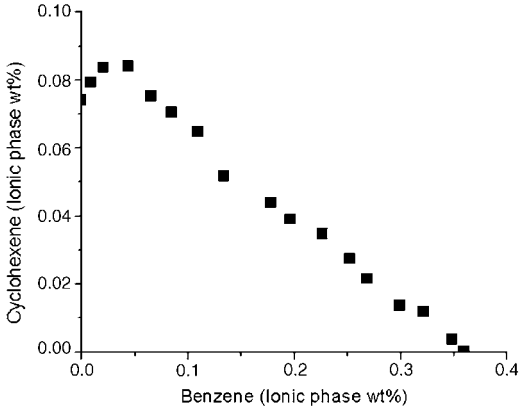

Figure 2. Benzene and cyclohexene contents in the ionic phase at 75 °C in a benzene/cyclohexene/BMI·PF_6.

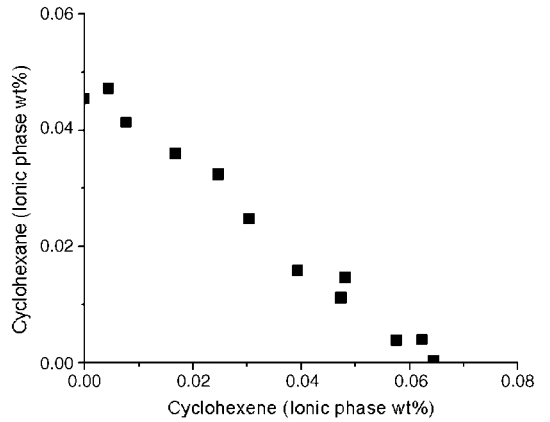

Figure 3. Cyclohexane and cyclohexene contents in the ionic phase at 75 °C in a cyclohexene/cyclohexane/BMI·PF_6.

Preparation and characterisation of nanoscale Ru^0 particles: Among the various methods available for the generation of Ru^0 nanoparticles,[11] the controlled decomposition of orga-

Abstract in Portuguese: *A decomposição controlada de complexos organometálicos de Ru^0 dispersos nos líquidos iônicos hexafluorofosfato de 1-n-butil-3-metilimidazólio (BMI·PF_6), tetrafluoroborato de 1-n-butil-3-metilimidazólio (BMI·BF_4) ou triflato de 1-n-butil-3-metilimidazólio (BMI·CF_3SO_3) na presença de H_2 representam um método simples e eficiente para a geração de nanopartículas de Ru^0. Análises de microscopia eletrônica de transmissão indicam a formação de superestruturas com tamanho aproximado de 57 nm formadas por nanopartículas dispersas de Ru^0 com diâmetro entre 2.6 ± 0.4 nm. Estas nanopartículas dispersas em líquidos iônicos são catalisadores multifase eficientes para a hidrogenação de alquenos e benzeno em condições reacionais suaves (4 atm, 75 °C). O diagrama ternário de (benzeno/ciclo-hexeno/BMI·PF_6) indica uma concentração máxima de 1% de ciclo-hexeno em BMI·PF_6, atingida com 4% de benzeno na fase iônica. Estas diferenças de solubilidade no líquido iônico podem ser exploradas para a extração de ciclo-hexeno durante a hidrogenação de benzeno por catalisadores de Ru dispersos em BMI·PF_6. Seletividades superiores a 39% em ciclo-hexeno podem ser obtidas a baixas conversões benzeno. Embora o rendimento máximo de 2% em ciclo-hexeno é bastante baixo para uma aplicação prática, este caso representa um exemplo raro de hidrogenação parcial de benzeno por nanopartículas solúveis de metais de transição.*

nometallic compounds developed by Chaudret is one of the most simple and effective.[12] Thus, Ru nanoparticles of a controlled size were easily prepared by the controlled decomposition of [Ru(cod)(cot)] (cod = 1,5-cyclooctadiene, cot = 1,3,5-cyclooctatriene), dissolved in pure alcohols or alcohol/THF mixture, with molecular hydrogen.[12] In this context, imidazolium ionic liquids[8,13] (shown here) provide a unique medium for the preparation and stabilisation of Ir^0, Rh^0, Pd^0 and Pt^0 particles with small diameters (2–3 nm) and a narrow size distribution.[14] Therefore, it was of interest to check whether these liquids could provide a suitable environment for the syntheses and stabilisation of Ru^0 nanoparticles by means of Chaudret's approach.

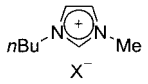

X=BF_4: BMI.BF_4
X=PF_6: BMI.PF_6
X=CF_3SO_3: BMI.CF_3SO_3

Thus, the treatment of a yellow suspension of [Ru(cod)(cot)] in 1-*n*-butyl-3-methylimidazolium hexafluorophosphate (BMI·PF_6), tetrafluoroborate (BMI·BF_4) or trifluoromethane sulfonate (BMI·CF_3SO_3) ionic liquids with molecular hydrogen (4 atm) at 75 °C for 18 h affords a black solution. The black solid material isolated from this solution by centrifugation was washed with acetone and dried under reduced pressure.

XRD powder analysis indicated that the solid consists of metal particles of hexagonal close packed (hcp) ruthenium. The Bragg reflections corresponding to crystalline ruthenium particles were observed at $2\theta = 37.76$, 42.05, 43.43, 57.78, 68.17, 77.80, 83.48 and 84.38°, which correspond to the indexed planes of the (hcp) crystals of Ru^0: (100), (002), (101), (102), (110), (103), (112) and (201), respectively. The most representative reflections of Ru^0 were indexed as hexagonal with unit cell parameters $a = 2.7487$ and $c = 4.2937$ Å. The mean diameter of the Ru particles, calculated with Scherrer's equation, is ≈ 2.5 nm, which is in good agreement with the TEM results (see later). Moreover, energy dispersion spectrometry (EDS) indicates the presence of Ru^0 and selected area diffraction (SAD) produces ring patterns that can be fitted to a simulation based on Ru^0 parameters (see the Supporting Information). Note that all the samples display the same spectrum, independent of the ionic liquid used (BMI·PF_6, BMI·BF_4 of BMI·CF_3SO_3) for their preparation.

However, X-ray photoelectron spectroscopy (XPS) of a sample shows oxidised ruthenium and oxygen peaks that indicate the presence of a passivated surface layer. However, the Ru–O components disappear almost completely after sputtering with Ar^+; this shows that only the external surface ruthenium atoms were oxidised (Figure 4). The same behaviour was observed by Chaudret for Ru^0 nanoparticles prepared in the presence of pure alcohols or alcohol/THF mixtures.[12] Moreover, the ease with which the surface atoms are oxidised is a general trend for ruthenium particles.[15] It is interesting to note that only the peaks corresponding to carbon (support), ruthenium and oxygen were observed. Note that the Ru $3d_{3/2}$ peak appears to be more intense owing to the superposition with the carbon 1s signal (Figure 4).

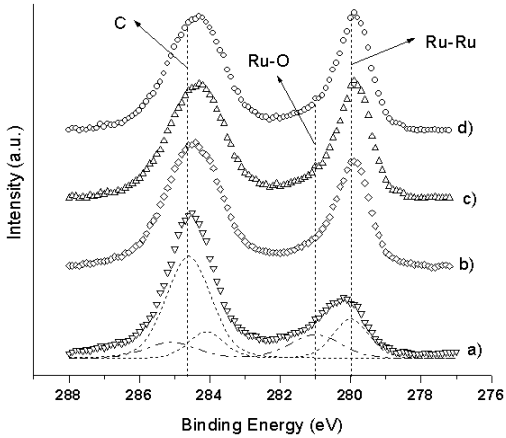

Figure 4. XPS surface survey of the Ru nanoparticles (Ru–Ru and Ru–O BE region) before and after sputtering with Ar^+.

The ruthenium nanoparticles were also examined by transmission electron microscopy (TEM). TEM observations show the formation of spherical superstructures of Ru particles with a regular size of 57 ± 8 nm (Figure 5a and b).

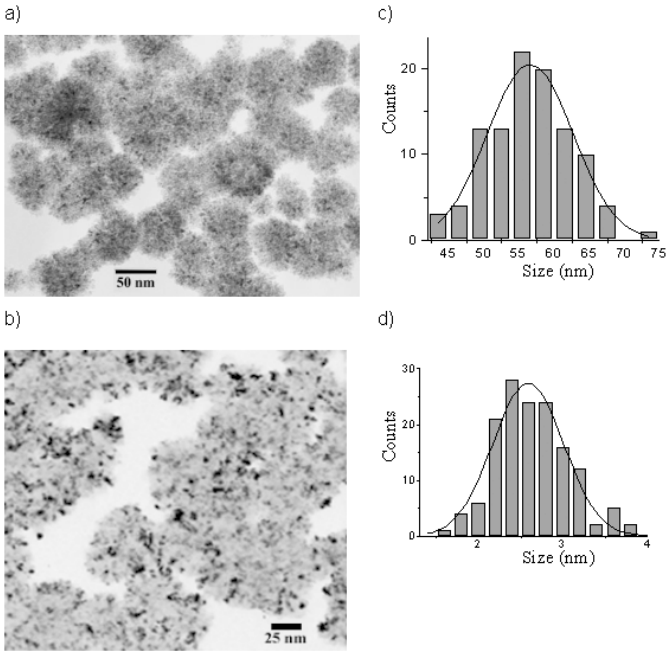

Figure 5. Images of the Ru nanoparticles prepared in BMI·PF_6 showing a) the superstructures (bar = 50 nm), b) inside the spherical superstructures (bar = 25 nm), and c, d) the corresponding histograms.

A mean diameter of 2.6 ± 0.4 nm for the Ru^0 nanoparticles present inside the superstructures was estimated from ensembles of 150 particles found in arbitrary chosen areas of the enlarged micrographs of five superstructures. Figure 5c and d show the obtained particle size distributions, which can be fitted reasonably well to a Gaussian curve. The same type of superstructure was found for Ru particles prepared in a MeOH/THF mixture; however, the size of the Ru nanoparticles could be not determined on account of their close proximity.[12]

Hydrogenation of olefins and arenes: We first investigated the catalytic properties of these nanoparticles re-dispersed in the ionic liquids as a stable black "solution" or in solventless conditions with respect to the hydrogenation of alkenes and benzene (Table 1).[16,17]

The data in Table 1 indicate that the Ru nanoparticles act as a relatively highly active catalyst for both multiphase and solventless hydrogenation of 1-hexene, cyclohexene and 2,3-dimethyl-2-butene (see entries 1–8) under mild reaction conditions. The Ru^0 nanoparticles dispersed in the ionic liquid seem to be quite stable under the reaction conditions, and the recovered ionic liquid catalytic solution (Table 1, entry 2) could be re-used at least 8 times without any significant changes in the catalytic activity for the 1-hexene hydrogenation. Moreover, TEM analysis of the particles embedded in the ionic liquid after benzene hydrogenation shows the same average size (2.6 ± 0.4 nm) and size distribution (Figure 6).

It is also clear from the data in Table 1 that the reactions performed under solventless conditions are faster than those performed with the particles dispersed in the ionic liquids, particularly for the cyclohexene and benzene hydrogenations (compare entry 4 with 5 and 6, and entry 8 with 9–11, Table 1). This difference is attributed to the typical multiphase conditions of the reactions performed in the ionic liquids; this can be a mass-transfer-controlled process.[18]

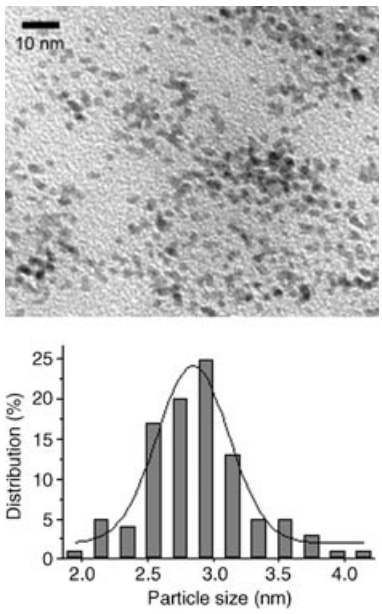

Figure 6. TEM micrograph of ruthenium nanoparticles embedded in BMI·BF_4 after hydrogenation of benzene under biphasic standard conditions (bar = 10 nm). Histogram illustrating the particle size distribution.

Table 1. Hydrogenation of alkenes and arenes by Ru^0 nanoparticles under multiphase and solventless conditions (75 °C and 4 atm, constant pressure, substrate/Ru = 500).

Entry	Medium	Substrate	t [h]	Conversion [%]	TON[a]	TOF [h^{-1}][b]
1	solventless	1-hexene	0.7	>99	500	714
2	BMI·BF_4	1-hexene	0.6	>99	500	833
3	BMI·PF_6	1-hexene	0.5	>99	500	1000
4	solventless	cyclohexene	0.5	>99	500	1000
5	BMI·BF_4	cyclohexene	5.0	>99	500	100
6	BMI·PF_6	cyclohexene	8.0	>99	500	62
7	solventless	2,3-dimethyl-2-butene	1.2	76	380	316
8	solventless	benzene	5.5	90	450	82
9	BMI·BF_4	benzene	17.3	30	150	9
10	BMI·PF_6	benzene	18.5	73	365	20
11	BMI·CF_3SO_3	benzene	17.5	50	240	14
12	solventless	benzene[c]	2.0	>99	250	125
13	solventless	toluene[c]	5.6	>99	250	45
14	solventless	isopropylbenzene[c]	6.4	>99	250	39
15	solventless	*tert*-butylbenzene[c]	14.1	>99	250	18
16	solventless	anisole	18	<1	–	–

[a] Turnover number TON = mol of hydrogenated product/mol of Ru. [b] Turnover frequency TOF = TON/h. [c] Arene/Ru = 250.

The catalytic activity attained under either solventless or multiphase conditions for this reaction is far superior to that of Ru nanoparticles prepared in alcohols/THF mixture. A TON (TON = turnover number) of 48 was obtained in the benzene hydrogenation after 6 days at 80 °C and 5 atm of H_2.[12b] The hydrogenation of alkyl benzenes catalysed by the Ru nanoparticles in solventless conditions (arene/Ru = 250, 75 °C, 4 atm) is sensitive to the to steric bulk of the alkyl group (Table 1, entries 12–14 and Figure 7). The initial TOF for 20% arene conversion was 122, 55, 43 and 35 h^{-1} for the benzene, toluene, isopropylbenzene and *tert*-butylbenzene hydrogenation, respectively.

It is also worth noting that the Ru nanoparticles are only marginally active for the hydrogenation of anisole (Table 1, entry 16) under the standard reaction conditions (4 atm, 75 °C).

Partial hydrogenation of benzene to cyclohexene: The catalytic tests for the partial hydrogenation of benzene to cyclohexene were performed with Ru nanoparticles and with a supported Ru catalyst (Ru/Al_2O_3, 5%, Strem) under solventless and multiphase conditions (entries 8–11, Table 2).

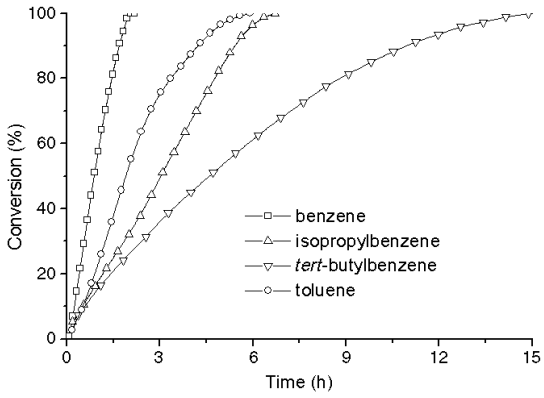

Figure 7. Compared hydrogenation of arenes under solventless conditions by Ru^0 nanoparticles [4 atm of H_2 (constant pressure) at 75 °C, arene/Ru = 250].

Table 2. Partial hydrogenation of benzene by Ru^0 nanoparticles and supported Ru/Al_2O_3 catalysts under ionic liquid and solventless conditions (75 °C, constant hydrogen pressure, benzene/Ru = 1500).

Entry	Catalyst/Medium	P [atm]	t [h]	Conversion [%]	Selectivity [%][a]	TON[b]
1	$[Ru^0]_n$/BMI·PF_6	4	2.0	10	15	150
2	$[Ru^0]_n$/BMI·PF_6	4	4.5	22	7	330
3	$[Ru^0]_n$	4	1.0	9	4	135
4	$[Ru^0]_n$	4	2.7	19	2	285
5	Ru/Al_2O_3	6	0.4	2	7	30
6	$[Ru^0]_n$	6	0.7	8	1	120
7	$[Ru^0]_n$	6	2.9	17	<1	255
8	Ru/Al_2O_3	6	1.0	6	<1	90
9	$[Ru^0]_n$/BMI·PF_6	6	1.2	2	34	30
10	$[Ru^0]_n$/BMI·PF_6	6	4.5	7	21	105
11	$[Ru^0]_n$/BMI·PF_6	6	27.7	15	11	225
12	Ru/Al_2O_3/BMI·PF_6	6	4.1	3	15	45
13	Ru/Al_2O_3/BMI·PF_6	6	5.5	6	9	90
14	Ru/Al_2O_3/BMI·PF_6	6	21.2	11	5	165
15	$Ru/Al_2O_3/H_2O$	6	0.7	7	<1	105
16	$Ru/Al_2O_3/H_2O$	6	1.5	17	<1	255
17	$[Ru^0]_n/H_2O$	6	0.5	8	1	120
18	$[Ru^0]_n/H_2O$	6	1.2	17	<1	255

[a] Selectivity in cyclohexene. [b] Turnover number TON = mol of hydrogenated products (cyclohexene and cyclohexane)/mol of Ru.

It is clear that for both Ru catalysts the best cyclohexene selectivity was attained in the reactions performed in the presence of the ionic liquid (compare entries 1 and 2 with 3 and 4). It is also evident that in BMI·PF_6 the best cyclohexene selectivity is achieved with the Ru^0 nanoparticles compared to the supported Ru catalysts at any benzene conversion (compare 9–11 with 12–14, Table 2). This result is in agreement with what was observed earlier, namely, that nonsupported Ru catalysts are more effective than supported ones.

It is also interesting to note that the addition of water to the ionic phase causes the partial decomposition of the imidazolium ionic liquid,[14] and the selectivity in cyclohexene drops to ≈1% at 3% benzene conversion.

In the case of Ru^0 nanoparticles in BMI·PF_6, a maximum of 39% selectivity at 1% benzene conversion was obtained. This drops to 11% at 15% benzene conversion (Figure 8).

It is reasonable to assume that the cyclohexene selectivity of hydrogenation processes in the ionic liquid phase for both Ru catalysts investigated is not only a consequence of the different cyclohexene/benzene solubility in BMI·PF_6, but, in these cases, the BMI·PF_6 can act as a reaction modifier (similar to the process in water).[6] It is worth noting that the selectivity attained in cyclohexenes for the hydrogenation of alkyl benzenes (Figure 7 and entries 13–15, Table 1) was less than 2%, even at very low arene conversions. This is probably related to the hydrogenation rate of these arenes, which are very low compared to the benzene.

The selectivity in cyclohexene attained in the benzene hydrogenation catalysed by Ru^0 nanoparticles in BMI·PF_6 is reasonable (up to 39% at 1% benzene conversion). However, the cyclohexene yields achieved so far (2%) are too low for technical application (compared, for example, to the industrial nonsupported Ru catalysts suspended in aqueous phase that can reach 60% yield).[19] Nevertheless, these values of cyclohexene selectivity and yield are similar to those observed for the gas-phase hydrogenation of benzene catalysed by supported Ru catalysts.[7] Catalysts based on soluble transition-metal nanoparticles that promote the selective reduction of benzene to cyclohexene are very rare. For example, cyclohexenes were observed in the hydrogenation of sterically bulky arenes, such as 1,2,4,5-tetramethylbenzene, by Rh^0 nanoparticles in an aqueous biphasic system[20] and in the partial hydrogenation of anisole by the use of polyoxoanions and tetrabutylammonium-stabilised Rh^0 nanoclusters (an initial selectivity of 30% in 1-methoxycyclohexene was observed at low anisole conversions).[21]

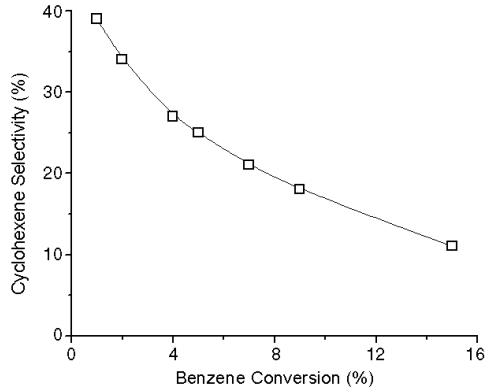

Figure 8. Cyclohexene selectivity in the hydrogenation of benzene by Ru^0 nanoparticles in BMI·PF_6 (6 atm of H_2 at 75 °C).

Conclusion

We have shown that stable Ru^0 nanoparticles can be easily prepared by simple decomposition of [Ru(cod)(cot)] dispersed in imidazolium ionic liquids. The ternary diagram (benzene/cyclohexene/BMI·PF_6) indicates that a maximum of 1% cyclohexene concentration in BMI·PF_6 is attained at a 4% benzene concentration in the ionic phase. This difference in solubility in the ionic liquid can be used for the extraction of cyclohexene during the hydrogenation of benzene by Ru catalysts suspended in BMI·PF_6. A selectivity of <39% in cyclohexene can be attained at very low benzene conversion by the use of nanoscale Ru particles. However, the cyclohexene yield and selectivity achieved so far are too low for technical applications and are much lower than those obtained by Ru catalysts suspended in water.

Experimental Section

General methods: All reactions involving ruthenium compounds were carried out under an argon atmosphere in oven-dried Schlenk tubes. The ionic liquids BMI·PF_6, BMI·BF_4 and BMI·CF_3SO_3 were prepared according to known procedures[22] and dried over molecular sieves (4 Å). Their purity was checked by an $AgNO_3$ test, ^1H and ^{31}P NMR spectroscopy, cyclic voltammetry (water ($<0.1\%$ v/v) and chloride content ($<1.8\,mg\,L^{-1}$)).[23] Solvents and arenes were dried with appropriate drying agents and distilled under argon prior to use. [Ru(cod)(cot)] was prepared by reduction of $RuCl_3$ with Zn in the presence of 1,5-cyclooctadiene following a known procedure.[24] All other chemicals were purchased from commercial sources and used without further purification. NMR spectra were recorded on a Varian Inova 300 spectrometer. Mass spectra were recorded on a GC/MS Shimadzu QP-5050 (EI, 70 eV). Gas chromatography analyses were performed on a Hewlett-Packard 5890 gas chromatograph with a FID and 30 m capillary column with a dimethylpolysiloxane stationary phase. The powder X-ray diffraction was performed in a Philips X'Pert MRD diffractometer. The diffraction data were collected at room temperature in a Bragg–Brentano geometry with a curved graphite crystal as the monochromator. The equipment was operated at 40 kV and 40 mA with a scan range between 20° to 100°. Transmission electron microscopy (TEM) was performed on a JEOL 2010 microscope operating at 200 kV and with a nominal resolution of 0.25 nm.

The synthesis of the nanoparticles and their hydrogenation reactions were carried out in a modified Fischer–Porter bottle immersed in a silicon oil bath and connected to a hydrogen tank. The drop in the hydrogen pressure in the tank was monitored with a pressure transducer interfaced through a Novus converter to a PC. The data was processed with Microcal Origin 5.0 (adapted from reference [6k]). The temperature was maintained at 75 °C by a hot stirring plate connected to a digital controller (ETS-D4 IKA). Controlled stirring at 800 rpm was used (no ionic catalytic solution projection was observed). The catalyst/substrate ratio was calculated from the initial quantity of $[Ru^0]_n$ used.

Formation and isolation of nanoparticles: In a typical experiment, a Fischer–Porter bottle containing a yellow suspension of [Ru(cod)(cot)] (92.5 mg, 0.3 mmol) in one of the ionic liquids BMI·PF_6, BMI·BF_4 and BMI·CF_3SO_3, 7 mL) was treated with 4 atm of H_2 at 75 °C to afford a black solution after stirring for 18 h. The Ru nanoparticles were isolated by centrifugation (3000 rpm) for 30 minutes, washed with water (5 × 15 mL) and acetone (5 × 15 mL), and then dried under reduced pressure. The Ru samples thus obtained were prepared for TEM, XPS and XRD powder analysis, and for catalytic experiments (see below).

Hydrogenation reactions:

Liquid–liquid biphasic: The olefins or benzene were added to the ionic catalytic solution obtained by dispersion of the isolated Ru nanoparticles (described above) in the ionic liquid (1 mL) and hydrogen was admitted to the system at 4 or 6 atm (constant pressure). Samples for GC and GC-MS analysis were also removed from time to time under H_2. The reaction mixture forms a typical two-phase system (the lower phase contained the Ru nanoparticles in the ionic liquid and the upper phase the organic products). The organic phase was separated by decantation or distillation, and was then weighed and analysed by GC, GC-MS and ^1H NMR spectroscopy.

Solventless: The isolated nanoparticles were placed in a Fischer–Porter bottle, and the arene was added. The reactor was placed in an oil bath at 75 °C, and hydrogen was admitted to the system at constant pressure (4 or 6 atm). Samples for GC and GC-MS analysis were also removed from time to time under H_2. The organic products were recovered by simple filtration and analysed by GC.

Identification of cyclohexene in the hydrogenation of benzene: The identification of cyclohexene was unequivocally established by GC-MS and by GC retention time versus an authentic sample of cyclohexene (Acros). GC was performed in a 100 m capillary column with a dimethylpolysiloxane stationary phase (0.25 mm × 0.5 μm). The GC parameters were: initial temperature 100 °C, initial time 30 min, temperature ramp 25 °C min^{-1}, final temperature 250 °C, detector and injector port temperature 250 °C and injection volume 1 μL.

Transmission electron microscopy: Transmission electron microscopy (TEM) observations and selected area diffraction patterns were taken on a JEM-2010 microscope operating at an accelerating voltage of 200 kV. Samples for TEM observations were prepared by placing a thin film of the ruthenium nanoparticles dispersed in isopropanol in a holed carbon grid. The size distribution of the metal particles was determined from the measurement of ≈150 particle, assuming spherical shape, found inside five superstructures.

Sample preparation and XRD powder analysis: The thin 1.0 mm layer of Ru powder was deposited into a small cavity on a glass substrate covered with a Kapton tape. The diffraction pattern was obtained after subtraction of the powder spectrum from a background measured with a glass substrate plus Kapton tape. The WAXD pattern confirmed crystalline Ru^0 by indexation of Bragg reflections obtained by a pseudo-Voigt profile fitting using the FULLPROF code. The most representative reflections to Ru^0 were indexed as hexagonal and the cell unit parameters obtained were $a=2.7487$ and $c=4.2937$ Å. The Bragg reflections at 37.76, 42.05, 43.43, 57.78, 68.17, 77.80, 83.48 and 84.38° correspond to the indexed planes of the (hcp) of Ru^0 crystals: (100), (002), (101), (102), (110), (103), (112) and (201). The mean diameter of the ruthenium particles was estimated to be 2.5 nm by means of the Debye–Scherrer equation[25] and assuming spherical particles.

X-ray photoelectron spectroscopy (XPS): XPS was performed with Mg_K radiation ($h\nu=1253.6$ eV). High-resolution scans were recorded with a pass energy of 15 eV, an angular acceptance of ±4° and an entrance slit of 2 mm diameter with an Omicron EA 125 hemispheric analyser. The detection angle, θ, of the photoelectrons with respect to the normal to the sample surface (takeoff angle) was 45°. Samples for analysis were prepared by placing the Ru nanoparticles on a conducting carbon tape. In addition to the C peaks (support), only Ru and O were observed (special monitoring the presence of other possible elements such as chloride or fluoride was not detected).

Phase diagrams: The three ternary diagrams C_6H_6/C_6H_{10}/BMI·PF_6, C_6H_6/C_6H_8/BMI·PF_6 and C_6H_8/C_6H_{10}/BMI·PF_6 were determined by a gravimetric method. Known quantities of each component were added to a centrifuge tube, and the system was stirred at 75 °C for ≈30 min. The upper phase was then separated from the system and its mass and composition determined by GC (no significant amount of the ionic liquid in the organic phase was observed). The composition of the lower phases was determined by component mass balance, namely, the lever-arm rule for biphasic systems. Each experiment was repeated at least three times in order to ensure the reproducibility of the method.

Acknowledgments

We thank CNPq, FAPERGS, CTPETRO, CAPES and CENPES-Petrobras for financial support.

[1] *Applied Homogeneous Catalysis with Organometallic Compounds* (Eds.: B. Cornils, W. A. Herrmann), Wiley-VCH, Weinheim, **1996**.

[2] a) B. Cornils, *Angew. Chem.* **1995**, *107*, 1709; *Angew. Chem. Int. Ed. Engl.* **1995**, *34*, 1575; b) *Aqueous-Phase Organometallic Catalysis, Concepts and Applications* (Eds.: B. Cornils, W. A. Herrmann), Wiley-VCH, Weinheim, **1996**.

[3] For recent reviews, see: a) C. Baudequin, J. Baudoux, J. Levillain, D. Cahard, A.-C. Gaumont, J.-C. Plaquevent, *Tetrahedron: Asymmetry* **2003**, *14*, 3081; b) C. E. Song, *Chem. Commun.* **2004**, 1033; c) J. Dupont, R. F. de Souza, P. A. Z. Suarez, *Chem. Rev.* **2002**, *102*, 3667; d) H. Olivier-Bourbigou, L. Magna, *J. Mol. Catal. A: Chem.* **2002**, *182*, 419; e) P. J. Dyson, *Transition Met. Chem.* **2002**, *27*, 353; f) C. M. Gordon, *Appl. Catal. A* **2001**, *222*, 101; g) R. Sheldon, *Chem. Commun.* **2001**, 2399; h) P. Wasserscheid, W. Keim, *Angew. Chem.* **2000**, *112*, 3926; *Angew. Chem. Int. Ed.* **2000**, *39*, 3772; i) J. Dupont, C. S. Consorti, J. Spencer, *J. Braz. Chem. Soc.* **2000**, *11*, 337.

[4] a) A. Roucoux, J. Schulz, H. Patin, *Chem. Rev.* **2002**, *102*, 3757; b) H. Bonnemann, R. M. Richards, *Eur. J. Inorg. Chem.* **2001**, 2455.

[5] T. Printz, W. Keim, B. Driesen-Hollscher, *Angew. Chem.* **1996**, *108*, 1835; *Angew. Chem. Int. Ed. Engl.* **1996**, *35*, 1708.
[6] For liquid-phase hydrogenations, see for example: a) L. Ronchin, L. Toniolo, *Appl. Catal. A* **2001**, *208*, 77; b) S. Xie, M. Qiao, H. Li, W. Wang, J.-F. Deng, *Appl. Catal. A* **1999**, *176*, 129; c) Z. Liu, W.-L. Daí, B. Liu, J.-F. Deng, *J. Catal.* **1999**, *187*, 253; d) S.-C. Hu, Y.-W. Chen, *Ind. Eng. Chem. Res.* **2001**, *40*, 6099; e) S.-C. Hu, Y.-W. Chen, *Ind. Eng. Chem. Res.* **2001**, *40*, 3127; f) S.-C. Hu, Y.-W. Chen, *Ind. Eng. Chem. Res.* **1997**, *36*, 5153; g) S.-C. Hu, Y.-W. Chen, *J. Chem. Technol. Biotechnol.* **2001**, *76*, 954; h) P. T. Suryawanshi, V. V. Mahajani, *J. Chem. Technol. Biotechnol.* **1997**, *69*, 154; i) C. Milone, A. Donato, M. G. Musolino, L. Mercadante, *J. Catal.* **1996**, *159*, 253; j) J. Struijk, J. J. F. Scholten, *Appl. Catal. A* **1992**, *82*, 277; k) J. Struijk, M. d'Angremond, W. J. M. L. Reget, J. J. F. Scholten, *Appl. Catal. A* **1992**, *83*, 263; l) S. Niwa, F. Mizukami, S. Isoyama, T. Tsuchiya, K. Shimizu, S. Imai, J. Imamura, *J. Chem. Technol. Biotechnol.* **1986**, *36*, 236; m) H. Nagahara, M. Konishi, US Patent 4734536 to Asihi Chem. Co. (**1988**).
[7] For gas-phase hydrogenations, see for example: a) J. Patzlaff, J. Gaube, *Chem. Eng. Technol.* **1998**, *21*, 651; b) E. Dietzsch, P. Claus, D. Hönicke, *Top. Catal.* **2000**, *10*, 99.
[8] a) Y. Chauvin, L. Mussmann, H. Olivier, *Angew. Chem.* **1995**, *107*, 2491; *Angew. Chem. Int. Ed. Engl.* **1995**, *34*, 2698; b) C. S. Consorti, A. P. Umpierre, R. F. de Souza, J. Dupont, P. A. Z. Suarez, *J. Braz. Chem. Soc.* **2003**, *14*, 401.
[9] L. A. Blanchard, J. F. Brennecke, *Ind. Eng. Chem. Res.* **2001**, *40*, 287.
[10] U. Domañska, A. Marciniak, *J. Chem. Eng. Data* **2003**, *48*, 451.
[11] See, for example: a) W. Yu, M. Liu, H. Liu, X. Ma, Z. Liu, *J. Colloid Interface Sci.* **1998**, *208*, 439; b) M. Liu, W. Yu, H. Liu, *J. Mol. Catal. A.: Chem.* **1999**, *138*, 295; c) A. Miyazaki, K. Takeschita, K. Aika, Y. Nakano, *Chem. Lett.* **1998**, 361; d) Y. Wang, J. Ren, K. Deng, L. Gui, Y. Tang, *Chem. Mater.* **2000**, *12*, 1622; e) H. Hirai, Y. Nakao, T. Toshima, *J. Macromol. Sci. Chem.* **1979**, *13*, 727; f) L. N. Lewis, N. Lewis, *Chem. Mater.* **1989**, *1*, 106; g) A. Duteil, R. Quéau, B. Chaudret, R. Mazel, C. Roucau, J. S. Bradley, *Chem. Mater.* **1993**, *5*, 341; h) H. Bönnemann, W. Brijoux, R. Brinkmann, R. Fretzen, T. Jounsen, T. Köppler, P. N. Richter, *J. Mol. Catal.* **1994**, *86*, 129; i) J.-M. Planeix, N. Coustel, B. Coq, V. Brotons, P. S. Kumbhar, R. Dutartre, P. Geneste, P. Bernier, P. M. Ajayan, *J. Am. Chem. Soc.* **1994**, *116*, 7935; j) W. Tu, H. Liu, *J. Mater. Chem.* **2000**, *10*, 2207; l) S. Gao, J. Zhang, Y.-F. Zhu, C.-M. Che, *New J. Chem.* **2000**, *24*, 739; m) G. Viau, P. Toneguzzo, A. Pierrard, O. Acher, F. Fiévet-Vincent, F. Fiévet, *Scr. Mater.* **2001**, *44*, 2263; n) A. Spitaleri, P. Pertici, N. Scalera, G. Vitulli, M. Hoang, T. W. Turney, M. Gleria, *Inorg. Chim. Acta* **2003**, *352*, 61.
[12] a) O. Vidoni, K. Philippot, C. Amiens, B. Chaudret, O. Balmes, J. O. Malm, J. O. Bovin, F. Senocq, M. J Casanove, *Angew. Chem.* **1999**, *111*, 3950; *Angew. Chem. Int. Ed.* **1999**, *38*, 3736; b) K. Pelzer, O. Vidoni, K. Philippot, B. Chaudret, V. Colliere, *Adv. Funct. Mater.* **2003**, *13*, 118.
[13] a) P. A. Z. Suarez, J. E. L. Dullius, S. Einloft, R. F. de Souza, J. Dupont, *Polyhedron* **1996**, *15*, 1217; b) P. Bonhote, A. P. Dias, N. Papageorgiou, K. Kalyanasundaram, M. Gratzel, *Inorg. Chem.* **1996**, *35*, 1168.
[14] a) J. Dupont, G. S. Fonseca, A. P. Umpierre, P. F. P. Fichtner, S. R. Teixeira, *J. Am. Chem. Soc.* **2002**, *124*, 4228; b) G. S. Fonseca, A. P. Umpierre, P. F. P. Fichtner, S. R. Teixeira, J. Dupont, *Chem. Eur. J.* **2003**, *9*, 3263; c) C. W. Scheeren, G. Machado, J. Dupont, P. F. P. Fichtner, S. R. Teixeira, *Inorg. Chem.* **2003**, *42*, 4738; d) J. Huang, T. Jiang, B. X. Han, H. X. Gao, Y. H. Chang, G. Y. Zhao, W. Z. Wu, *Chem. Commun.* **2003**, 1654; e) L. M. Rossi, G. Machado, P. F. P. Fichtner, S. R. Teixeira, J. Dupont, *Catal. Lett.* **2004**, *92*, 149.
[15] a) R. Kikuchi, F. Mizukami, S. Niwa, M. Toba, H. Ushijima, K. Itou, *Appl. Catal.* **1997**, *165*, 309; b) H. Madhavaram, H. Idriss, S. Wendt, Y. D. Kim, M. Knapp, H. Over, J. Assmann, E. Löffler, M. Muhler, *J. Catal.* **2001**, *202*, 296.
[16] For arene hydrogenation by transition-metal complexes in ionic liquids, see: a) P. J. Dyson, D. J. Ellis, W. Henderson, G. Laurenczy, *Adv. Synth. Catal.* **2003**, *345*, 216; b) C. J. Boxwell, P. J. Dyson, D. J. Ellis, T. Welton, *J. Am. Chem. Soc.* **2002**, *124*, 9334; c) P. J. Dyson, D. J. Ellis, D. G. Parker, T. Welton, *Chem. Commun.* **1999**, 25.
[17] For a recent review in arene hydrogenation, see: P. J. Dyson, *J. Chem. Soc. Dalton Trans.* **2003**, 2964.
[18] S. S. Divekar, B. M. Bhanage, R. M. Deshpande, R. V. Gholap, R. V. Chaudhari, *J. Mol. Catal.* **1994**, *91*, L1–L5.
[19] H. Nagahara, M. Ono, M. Konishi, Y. Fukuoka, *Appl. Surf. Sci.* **1997**, *121/122*, 448.
[20] J. Blum, I. Amer, K. P. C. Vollhardt, H. Schwartz, G. Hohne, *J. Org. Chem.* **1987**, *52*, 2804.
[21] J. A. Widegren, R. G. Finke, *Inorg. Chem.* **2002**, *41*, 1558.
[22] J. Dupont, P. A. Z. Suarez, C. S. Consorti, R. F. de Souza, *Org. Synth.* **2002**, *79*, 236.
[23] a) B. K. Sweeny, D. G. Peters, *Electrochem. Commun.* **2001**, *3*, 712; b) V. Gallo, P. Mastrorilli, C. F. Nobile, G. Romanazzi, G. P. Suranna, *J. Chem. Soc. Dalton Trans.* **2002**, 4339.
[24] P. Pertici, G. Vitulli, *Inorg. Synth.* **1983**, *22*, 176.
[25] a) J. W. Niemantsverdriet *Spectroscopy in Catalysis*, VCH, Weinheim, **1995**; b) H. P. Klug, L. E. Alexander, *X-Ray Diffraction Procedures*, Wiley, New York, **1974**, Chapter 9.

Received: December 21, 2003
Published online: June 15, 2004

